

# High-Efficiency L and S-band Power Amplifiers with High-Breakdown GaAs-based pHEMTs

J. A. Pusl, R.D. Widman, J. J. Brown\*, M. Hu\*, N. Kaur, M. BeZaire, and L. D. Nguyen\*.  
Tel: (310) 416.4893, Fax: (310) 662.5198

Hughes Space and Communications Company EO/E4/P130  
P.O. Box 92919  
Los Angeles, CA 90009-2919

\*Hughes Research Laboratories MS RL-61  
3011 Malibu Canyon Road  
Malibu, CA 90265

## Abstract

Performance and reliability data for harmonically-terminated, high-efficiency microwave power amplifiers designed from active harmonic loadpull data utilizing high breakdown voltage AlGaAs/InGaAs/GaAs pHEMTs are reported. Single stage MIC amplifiers fabricated with 2x25 mm gate width pHEMTs resulted in  $P_{out}=20$  W and PAE=66% at 1.5 GHz and 2.2 GHz. Balanced hybrid amplifiers with these modules have been fabricated which have  $P_{out}=40$  W and PAE=64%. To the authors' knowledge, this is the highest combination of reliable output power and efficiency ever achieved with pHEMT devices. Single stage amplifiers fabricated with a single 5mm or 10 mm pHEMT gave  $P_{out}=2$  W and 4 W, respectively, with PAE=72%. All of these output powers are at power densities of 0.4 W/mm. These devices have undergone dc and RF lifetests with good results. This GaAs-based pHEMT device technology supports amplifier module designs in the 1-20 GHz frequency range.

## Introduction:

High efficiency power transistors are a critical building block of space-based, solid-state high-power amplifiers (HPAs, SSPAs). A large number of applications exist at L through K-bands (1-20 GHz). Competitive technologies that have demonstrated comparable but lower efficiency at L to C-band are GaAs MESFET and GaAs HFET. The GaAs-based pseudomorphic HEMT (pHEMT) promises the best high power, high efficiency performance [1-6]. One drawback to this technology has been low breakdown voltage [1-6], which affects device reliability. In this work, device data, amplifier design information, amplifier performance data, and reliability results obtained using a high-breakdown voltage pHEMT device technology [7-9] are reported.

## Device Structure:

The double-doped Al<sub>0.24</sub>Ga<sub>0.76</sub>As / In<sub>0.15</sub>Ga<sub>0.85</sub>As / GaAs pHEMT structure is grown by molecular beam epitaxy (MBE). This process has been described elsewhere [7-9]. The specific contact resistance is 0.25 ohm-mm. A source-drain spacing of 4 um and

channel recess width of 1.5 um were found to result in the best combined dc and RF performance. A unit gate finger width of 250 um was found to be optimum for L&S-band operation. The 0.3 um gates were formed by e-beam lithography and deposition of Ti/Pt/Au metalization. Silicon nitride was deposited (1000Å) for device passivation. The wafer was thinned to 50 um and backside vias were formed by wet chemistry. Devices were fabricated with total gate periphery of 0.5 mm to 25 mm.

Circuit	Freq. (MHz)	Pout (W) @ 7Vd-s	L-S gain (dB)	Avg. PAE (%)
L-driver	1525-1559	4	17	72
L-output	1525-1559	20	15	66
L-hybrid	1525-1559	40	15	64
S-driver	2170-2200	2	16	72
S-output	2170-2200	20	14	66

Table 1: Summary of L and S-band CW amplifier performance.

## Device and Amplifier Performance:

Figure 1 shows histograms of  $I_{max}$  and  $|BV_{gd}|$  for a recent wafer run. The dc data on these devices shows nominal  $I_{max}=470$  mA/mm (at  $V_{gs}=+1.0$  V), gate-drain breakdown voltage (source floating) of  $|BV_{gd}|=20$  V (measured at  $|I_{gd}|=0.1$  mA/mm; more conservative than the industry standard 1 mA/mm), and an operating transconductance of  $g_m=250$  mS/mm @ 100mA/mm. For all wafer lots,  $|BV_{gd}|$  for passivated devices was consistently in excess of 18 V, with some samples as high as 25 V. The repeatability and scaling of high breakdown voltage is a critical device parameter for performance and reliability.

S-parameters of the devices were measured and device models extracted. The gate-source capacitance,  $C_{gs}$ , is  $\sim 1$  pF/mm. The  $f_t$  of the process is nominally 30 GHz at  $V_{ds}=7$  V and 50 mA/mm (class AB) bias.

In-fixture power measurements were performed on 5 mm gate periphery devices using an active load-pull CW measurement system similar to the one reported in [10] at 1.5 and 2.2 GHz. The in-fixture (corrected to bond wire reference plane) measured output power ( $P_{out}$ ) and PAE was 2 W (0.4 W/mm) and >75%, respectively. In attaining the high PAE (approaching 80%), 2nd harmonic tuning and 3rd harmonic tuning improved PAE 8-10% and 2-3%, respectively. The data obtained with this measurement system assumes a conjugate input match for the device. When devices were tuned for higher output powers (0.5 W/mm), device PAE dropped to <70%. Our findings show that lower power densities (and the higher load impedances associated with them) at a given drain voltage are necessary to obtaining high PAE operation.

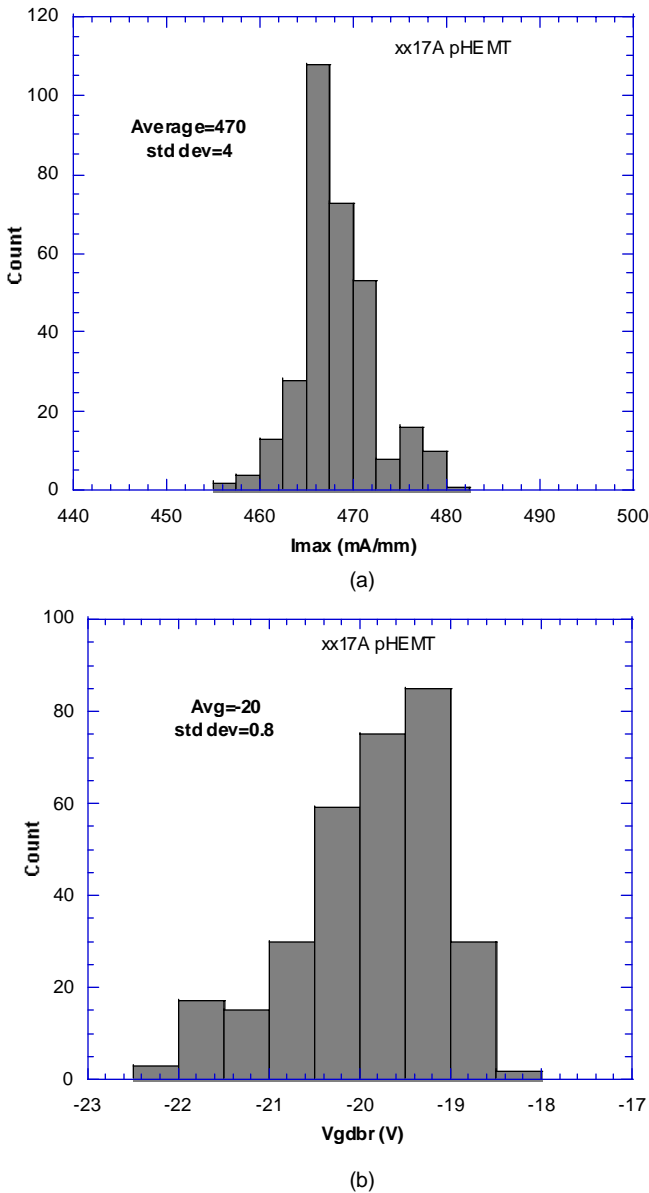


Figure 1: Histograms of (a) maximum channel current,  $I_{max}$  and (b) gate-drain breakdown,  $V_{gdrb}$  for a pHEMT wafer.

The load gammas measured for the 5 mm pHEMT at 2.185 GHz were 0.6 @ 160° for the 1<sup>st</sup> harmonic and large reflections ( $\Gamma > 0.9$ ) at +40° and -150° for the 2<sup>nd</sup> and 3<sup>rd</sup> harmonics, respectively. This set of impedances results in a (dominantly) class E amplifier. This type of amplifier is characterized by high impedance terminations at the higher harmonics, and a fundamental match such that the voltage and current waveforms switch completely out of phase. A lowpass output network was synthesized to give the same impedances as in the loadpull measurement. For the input matching network, a 2-pole lowpass design was implemented with an R-C damping network on the gate to make the amplifier critically stable in-band ( $1.1 < K < 1.5$ ,  $B_1 > 0$ ) and overdamped elsewhere. A photograph of the fabricated 5 mm S-band pHEMT driver amplifier is shown in Figure 2a.

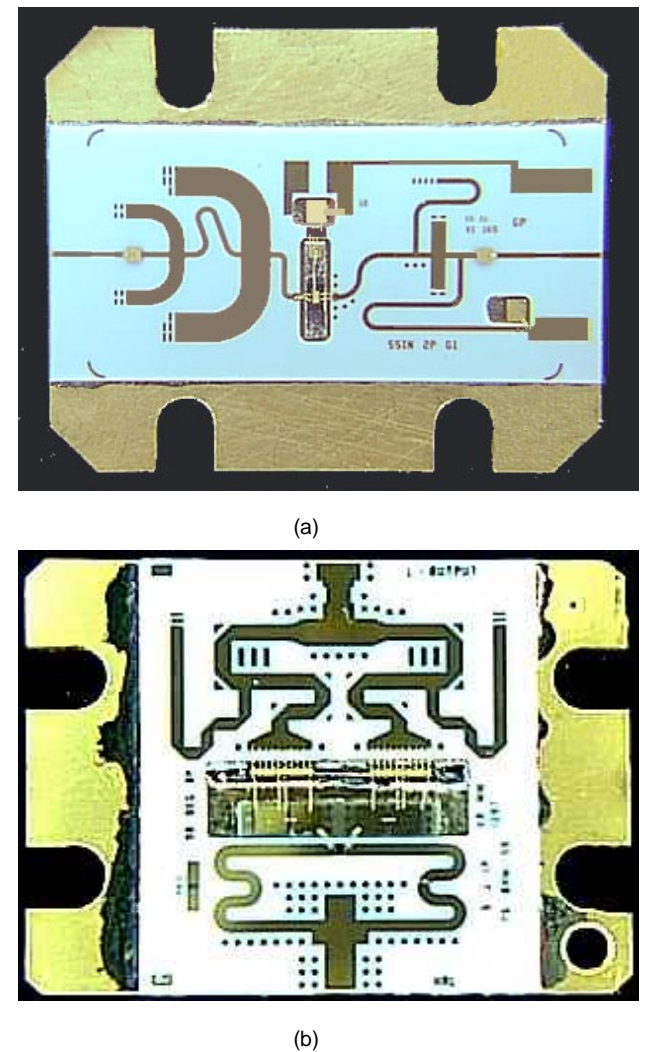


Figure 2: Photographs of two L&S-band pHEMT amplifiers: (a) shows a 2 W, S-band driver module and (b) a 20 W L-band output module.

For the 20 W designs (2x25 mm devices), the 5 mm fundamental loadpull impedance values were first transformed to the Cripps impedance [11] by adding the 5mm device drain-source capacitance,  $C_{ds}$ , in parallel and the drain series inductance and resistance ( $L_d$  and  $R_d$ ) in series. The scaled 50 mm values for  $C_{ds}$ ,  $L_d$ , and  $R_d$  were then removed from the Cripps impedance, for which a distributed network was synthesized. For the 2<sup>nd</sup> harmonic impedance, we attempted to reach the +40° phase angle of the loadpull measurement, and the closest we were able to realize in the space available was +90°. The unconditionally-stable amplifier has an input network with 1 pole (L-C lowpass) and a power divider. The 2x25 mm L-band output amplifier is shown in Figure 2b. The balanced 40 W design consists of 2 of the 20 W modules power combined by Duroid Wilkinson dividers with 90° of extra phase length in opposite 50 ohm feeds to balance the amplifier. The measured RF power performance of all the L and S-band designs is summarized in Table 1.

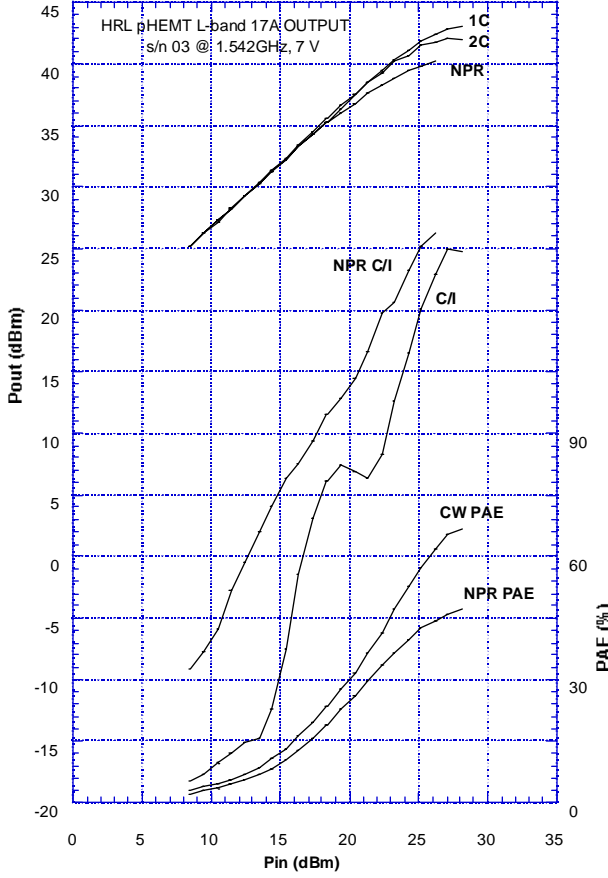


Figure 3: Measured large signal power and linearity curves for the 20 W L-band output amplifier.

Linearity measurements (two-tone (spacing=2 MHz) and noise-loaded (noise BW=34 MHz)) were made on the amplifiers. For the L-band output amplifier, the noise-loaded output power was

10.5 W at 14 dB NPR with 46% PAE (Figure 3). The output power and PAE vs. drain voltage is shown in Figure 4. This data shows an amplifier with output power of 16 W and ~70% PAE at 6 V. At 8 V, the data shows 22.5 W power out at 66% PAE.

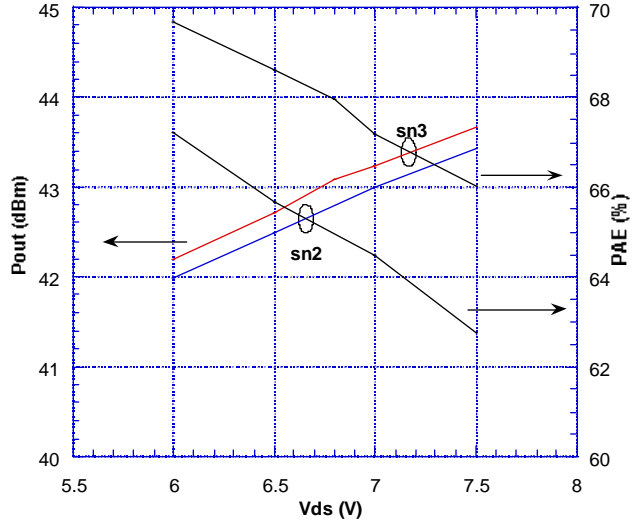
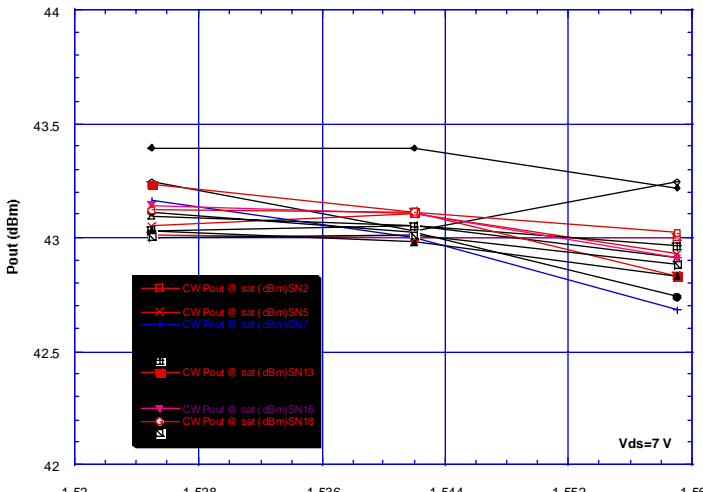


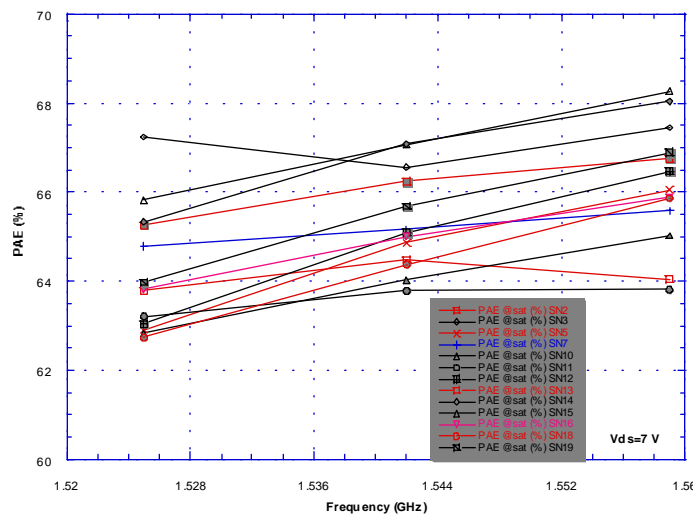
Figure 4: Output power and PAE vs.  $V_{ds}$  for two L-band "20 W" output amplifiers.

Thirteen 20 W L-band pHEMT amplifiers were assembled and measured with devices from 2 different wafer lots. Similar performance to that reported above was obtained for each of these amplifiers, with average  $P_{out}=20$  W and average PAE=65.5%, as seen in Figure 5.

On all of the designs, all MIC circuitry was printed. For devices of a given wafer, small adjustments were made to the basic design with either wire bonds across tuning pads or varying bond lengths on the semi-automatic bonder. Once the circuit was optimized for each wafer, all modules were assembled the same way. This procedure yielded optimal results with a minimum of circuit tuning. All of the quoted amplifier results were made in a system calibrated from coaxial connector to connector with  $V_{ds}$  measured external to the circuit.



(a)



(b)

Figure 5: Data showing output power (a) and PAE (b) for 13 of the L-band output amplifiers.

### Packaging:

We have developed low-cost, high performance packaging for our pHEMT amplifier modules. The base consists of a flat carrier of either Silvar-K or SiC/Al metal matrix composite. These materials have a CTE that is matched to alumina, while providing reasonable thermal characteristics ( $\sim 110$  W/mK for Silvar and  $\sim 180$  W/mK for SiC/Al MMC). The SiC/Al MMC material has the additional benefit of having a density similar to that of alumina. A single piece substrate of alumina with circuitry printed on it is soldered with AuGe to the carrier. Substrates have laser-drilled holes and filled vias as necessary. Figure 2 shows amplifiers constructed in this fashion. For device protection, bathtub-shaped lids made of alumina or plastic with epoxy seal rings are placed over the assembly.

### Reliability:

pHEMT devices and amplifiers have undergone dc and RF lifetests [9].

For the dc lifetest, 1 mm gate periphery devices were stressed at baseplate temperatures of 230°C and 250°C. The test conditions were such that the estimated average channel temperatures were  $\sim 30$ °C higher. DC reliability tests showed a MTTF at 250°C baseplate temperature of 2500 h. The 230°C baseplate tests are still ongoing, but based on current data, the activation energy is at least 1.2 eV. At 105°C, the MTTF is  $>2$ e7 h.

RF lifetests were conducted on C-band amplifiers built with devices from this same process. The C-band 2W amplifiers from [9] have been put on both ambient and elevated temperature (150°C baseplate) lifetests and have now accumulated  $\sim 200$ k device-hours. The amplifiers are being operated at voltages from  $V_{ds}=7$  to 9 V and  $\sim 3$  dB gain compression.  $P_{out}$  remains unchanged (i.e. no power slump has been observed).

RF step stress tests (steps in drain voltage) were conducted on the C-band 2 W amplifiers and the L-band 20 W amplifiers. Each step was either 500 or 1000 h. Results show that there is at least 2 V of drain voltage margin over our nominal operating  $V_{ds}$  of 7 V before any device degradation is experienced (i.e.  $V_{ds}=9$  V).

### Conclusions:

High breakdown voltage (20 V gate-drain @ 0.1 mA/mm), high-power GaAs-based pHEMT device technology for the 1-20 GHz frequency range has been reported. Fabricated L and S-band power amplifiers attained  $P_{out}=20$  W @ 0.4 W/mm with PAE  $>65\%$ . Hybrid combined 40 W L-band amplifiers with 64% PAE were demonstrated. To the authors' knowledge, this is the highest combination of output power and efficiency ever achieved with pHEMT devices. Multiple dc and RF lifetests have been completed with these devices/circuits and results indicate that they are reliable for space applications. These devices, circuits, and associated packaging are production-ready and available for insertion into our space-based solid state power amplifiers.

### References:

1. L. Aucoin, S. Bouthillette, A. Platzker, S. Shanfield, A. Bertrand, W. Hoke, P. Lyman, "Large Periphery, High Power Pseudomorphic HEMTs," 1993 GaAs IC Symp., pp. 351-353.
2. J. Shu, J. Wei, R. Basset, Y. Chung, C. Hua, C. Meng, P. Chye, J. Hall, D. Day, "C-band high- performance IMFETs and superIMFETs using MESFET and PHEMT technology for SATCOM applications," IEEE MTT-S Digest, 1994, pp. 561-564.
3. S. Bouthillette, A. Platzker, L. Aucoin, "High Efficiency 40 Watt PHEMT S-band MIC power amplifiers," IEEE MTT-S Digest, 1994 , pp. 667-670.

4. A. Platzker, S. Bouthillette, "Variable output, high efficiency-low distortion S-band power amplifiers...," IEEE MTT-S Digest, 1995, pp. 441-444.
5. S. Bouthillette, A. Platzker, "High efficiency L-band variable output power amplifiers...," IEEE MTT-S Digest, 1996, pp. 563-566.
6. J. Komiak, S. Wang, T. Rogers, "High efficiency 11 Watt octave S/C-band pHEMT MMIC power amplifier," IEEE MTT-S Digest, 1997, pp.1421-1424.
7. J. J. Brown, J. Josefowicz, A. E. Schmitz, M. Thompson, and C. E. Hooper, "Atomic Force Microscopy Structural Analysis for the Development of a Manufacturable HEMT Gate Recess Etch Process" GaAs Manufacturing Technology Conference, 1995, pp. 171-174.
8. J. J. Brown, J. A. Pusl, M. Hu, A. E. Schmitz, D. P. Docter, J. B. Shealy, M.G. Case, M. A. Thompson, and L.D. Nguyen, "High Efficiency GaAs-based pHEMT C-Band Power Amplifier," IEEE Microwave and Guided Wave Letters, Vol. 6, #2, 1996, pp. 91-93.
9. J. A. Pusl, J. J. Brown, J. B. Shealy, M. Hu, A. E. Schmitz, D. P. Docter, M.G. Case, M. A. Thompson, and L. D. Nguyen, "High-Efficiency GaAs-based Power Amplifier Technology for 1-18 GHz," IEEE MTT-S Digest, 1996, pp. 693-696.
10. B. Hughes, A Ferrero and A. Cognata, "Accurate on-wafer power and harmonic measurements of mm-wave amplifiers and devices," IEEE MTT-S Digest, 1992, pp. 1019-1022.
11. Cripps, S. C., "An introduction to high efficiency GaAsFET amplifier modes," Matcom, Inc. Technical note 3.5, (415) 493-6127.